European Journal of Wood and Wood Products (2020) 78:923–932
https://doi.org/10.1007/s00107-020-01570-5

ORIGINAL

Experimental and numerical evaluation of the structural performance of Uruguayan *Eucalyptus grandis* finger-joint

Abel Vega[1,2] · Vanesa Baño[1,3] · Andrea Cardoso[4] · Laura Moya[5]

Received: 27 September 2019 / Published online: 16 July 2020

Abstract
The aim of this study was to evaluate the structural performance of finger-joints made of Uruguayan *Eucalyptus grandis* and two types of adhesives. A numerical model for bending strength and stiffness prediction was developed. Model inputs were experimentally determined from tests on wooden specimens and from the literature. Finger-joints glued with two types of adhesives (one-component polyurethane -PUR- and emulsion polymer isocyanate-EPI-) were tested in bending and the failure modes were evaluated. Results show that adhesive type did not influence the stiffness of the finger-joint, but the bending strength. Specimens glued with PUR showed higher strength than those glued with EPI. A 3D model, using Comsol Multiphisic software, was developed to simulate the finger-joint behavior. Adhesive-wood interaction in the finger-joints was modelled using the Comsol Thin Elastic Layer module, defined by the elastic properties of the adhesives. The numerical results showed no differences on the stiffness of the joints regardless of adhesive type. Results agreed with those obtained from experimental tests, with a maximum error of 7%. Models predicted the bending strength with an error of 6% with respect to the experimental values. Different finger configurations were analysed, and the optimal geometry (20 mm-length, 6.2 mm-pitch and 1.0 mm-tip-thick) to attain the maximum strength for Uruguayan Eucalyptus was found.

1 Introduction

Glued laminated timber (GLT or glulam) is one of the most important engineered wood products (EWP) used at present in architecture and civil engineering. The manufacturing process is complex and involves many factors, such as species, adhesive type and applied pressure, among others. Optimum parameter combinations, both in glulam and lamella production, must be tailored to meet end-product´s requirements. The efficiency of the longitudinal assembly of laminations through suitable finger-joints is crucial for the overall structural performance of GLT and closely related to the manufacturing process. Production requirements for GLT and finger-joint have been well documented, and for softwood species and poplar are established in EN 14080 (CEN 2013). However, there are still several unknowns regarding finger jointing for hardwoods, or for new species/adhesives combinations. The influence of the manufacturing process on the mechanical properties of finger-joint hardwoods has been studied with emphasis on the production conditions such as timber conditioning (Raknes 1980), curing time and end pressure (Bourreau et al. 2013), finger-joint geometry (Ahmad et al. 2017; Özçifçi 2008; Ayarkwa et al. 2000a) and other several interlinked factors (Vrazel and Sellers Jr 2004). In addition, extensive literature related to the gluing performance and adhesive evaluation is available (Ayarkwa et al. 2000b; Vassiliou et al. 2006; Volkmer et al. 2014).

The principal criterion for structural finger-joint assessment is the load bearing strength, usually evaluated by static bending test. The test is considered as the most convenient for a preliminary study of finger joints and is commonly employed for quality control as well. Frequently, experimental programs are complemented with numerical simulations with the aim of modelling the mechanical behavior of finger joints. Finite element method (FEM) has been used for

✉ Vanesa Baño
vbanho@gmail.com

[1] Instituto de Estructuras Y Transporte, Facultad de Ingeniería, Universidad de La República, 11300 Montevideo, Uruguay

[2] CETEMAS, 33936 Carbayín, Spain

[3] CESEFOR, Timber Industry and Construction Area, 42005 Soria, Spain

[4] Laboratorio Tecnológico del Uruguay-LATU, 11500 Montevideo, Uruguay

[5] Facultad de Arquitectura, Universidad ORT Uruguay, 11300 Montevideo, Uruguay

simulation in analyses of wooden materials for over 30 years, due to the ability of dealing with the structural complexity of wood (Sebera et al. 2015), and has been reported as a convenient approach to model wooden materials when limited experimental data is available (Tran et al. 2014). Several researchers have successfully applied FEM to simulate the stress distribution in finger joints of softwood (Milner and Yeoh 1991; Serrano et al. 2001; Khelifa et al. 2015) and hardwood species (Smardzewski 1996; Tran et al. 2014; Franke and Marto 2014).

The main difficulty of finger-jointing hardwoods lies in the uncertainties of the wood-adhesive interaction. In particular, some species of *Eucalyptus* are not fully characterized, and therefore their interaction with some adhesives is still unknown. This is the case for Uruguayan fast-growing *Eucalyptus* spp. one of the most important renewable genera cultivated in Uruguay that covers more than 600,000 ha and produces annually approximately 11.2 million m^3 of roundwood. The major part is consumed by pulp and energy production, and 1.2 million m^3 from the annual average supply is intended for mechanical transformation (Dieste 2012). Having growth rates of 30 $m^3 ha^{-1}$ yr^{-1}, *Eucalyptus grandis* is a promising raw material for GLT production in Uruguay. Information on suitable adhesives for finger-jointing *Eucalyptus grandis* is scarce. The adhesive most commonly used for Eucalyptus glulam are phenoplast or aminosplast adhesives (Piter et al. 2007). However, in the last years, one-component polyurethane (PUR) and emulsion polymer isocyanate (EPI) adhesives are gaining acceptance for structural applications, and recently, they have been included in the European standards EN 14080 (CEN 2013) and EN 16351 (CEN 2015). Recently, few studies on glulam made of *Eucalyptus globulus* (Lara-Bocanegra et al. 2017; Franke and Marto 2014), *Eucalyptus grandis* (Moya et al. 2019; Bourscheid et al. 2015; Calil Neto et al. 2014) and a hybrid of two *Eucalyptus* species (Pereira et al. 2016) showed the potential of PUR with this genus. In general, the mechanical properties of glulam achieved values above those of the corresponding solid wood; however, certain difficulties related to the integrity of the glue line were also reported in these works. The literature on glulam made of hardwoods and EPI is limited; few works report on tropical species such as teak (Iwakiri et al. 2014) and beech (Volkmer et al. 2014). A study by Franke et al. (2014) comparing the finger joint performance of beech and PUR or beech and EPI, revealed no substantial difference in strength results.

In Argentina, the admissible teeth length (commonly 10 mm) (IRAM 2013a) is lower than that required in the European standards (CEN 2013), and the mechanical properties of GLT of *Eucalyptus grandis* (IRAM 2006) show values of bending strength lower than those of the corresponding solid wood (IRAM 2013b). In Uruguay, some companies commercialize non-structural glulam elements manufactured using finger-joint lengths of the laminations of approximately 13 mm, which are commonly used by builders as structural elements. Therefore, some research on the manufacturing of structural products of this species have been carried out (Moya et al. 2019).

Knowing the influence of the gluing quality on the successful performance of the finger-joint, several works have focused on analysing the adhesive-wood connection by models that simulate its behavior (Franke et al. 2014; Tran et al. 2014; Camú and Aicher 2018).

This study aims to evaluate the mechanical performance of finger-joints made of *Eucalyptus grandis* and two different adhesives, EPI and PUR, focusing on the bending properties and the glue line behavior. In addition, a numerical model to predict the modulus of elasticity and the bending strength of the finger-joints is presented.

2 Materials and methods

This study is divided into two phases: (i) an empirical testing program on physical sections cut from laminations, subjected to bending, and (ii) numerical modelling of the finger-jointed sections using input data from phase (i) tests.

2.1 Sampling

The material used in this study came from *Eucalyptus grandis* sawn boards that have been previously graded as Class 1 (IRAM 2013b), with corresponding values of 30 N/mm^2 for bending strength ($f_{m,k}$), 18 N/mm^2 for tension parallel to grain strength ($f_{t,0,k}$), 14 kN/mm^2 for longitudinal modulus of elasticity ($E_{0,mean}$), and 430 kg/m^3 for density (ρ_k).

In total, 80 specimens with a nominal cross section of 70 mm × 22 mm and 400 mm long were prepared from the selected boards and divided into three groups: (i) 40 with one finger-joint in the mid-span bonded with a bi-component adhesive, EPI (EPI WS742, WONDERBORD, MOMENTIVE); (ii) 20 with one finger-joint bonded with a single component polyurethane adhesive, PUR (PURBOND); and (iii) 20 control (without finger-joint). The last group was prepared to determine input values for the FE modelling, and to compare the effect of the finger-joint with different adhesives on the structural behavior of tested specimens.

All specimens were conditioned at 20 °C/65% RH until they reach values close to 12% moisture content. Finger-joints were then manufactured in the Technological Laboratory of Uruguay (LATU) following the production requirements described on EN 14080 (CEN 2013), with manual application of the adhesive and applying a clamping pressure of 10 MPa. The finger profile is shown in Fig. 1.

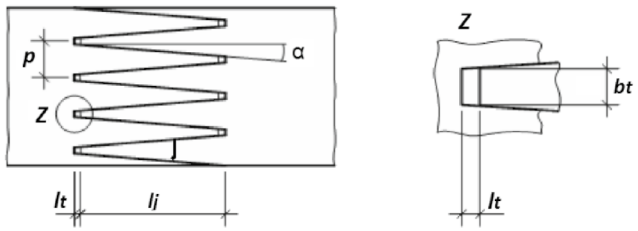

l_j	Finger length	15 mm
p	Pitch	4 mm
l_t	Tip gap	0,1 mm
b_t	Tip thickness	0,5 mm

Fig. 1 Finger-joint parameters (CEN 2013)

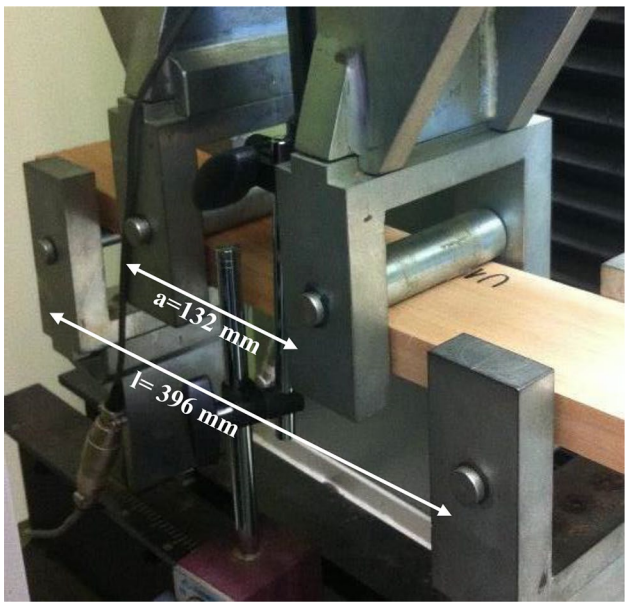

Fig. 2 4-point bending tests of the finger-joint in the universal bending machine Minebea

2.2 Testing

The specimens were tested in 4-point flatwise bending following the recommendations of EN 14080 (CEN 2013) and EN 408 (CEN 2010), with a span of 396 mm and two loads applied in the middle third of the length, as shown in Fig. 2. Values of modulus of elasticity were corrected to 12% MC according to EN 384 (CEN 2016a).

Modulus of elasticity and bending strength were calculated by Eqs. 1 and 2.

$$E_m = \frac{3al^2 - 4a^3}{2bh^3\left(2\frac{w_2 - w_1}{F_2 - F_1}\right)} \quad (1)$$

$$f_m = \frac{3Fa}{bh^2} \quad (2)$$

where h and b are the height and width of the specimen, respectively, in mm; a is the distance between one support and the nearest loading point (6 h), in mm; l is the span (18 h), in mm; F_1–F_2 is an increment of the load on the straight-line portion of the load deformation curve, in kN; w_1–w_2 is the increment of deformation corresponding to F_2–F_1, in mm; F is the maximum load at failure, in kN.

In addition, the failure mode of the finger joints was visually evaluated and roughly assigned to one of the following types: (i) mode 1, fracture occurs 100% by wood; (ii) mode 2, fracture partially occurs by wood and partially by adhesive; and (iii) mode 3, failure occurs 100% by adhesive. Figure 3 shows an example of each failure mode.

2.3 FE modelling

A 3D model, using Comsol Multiphysics software (Comsol Inc., USA), was developed to simulate the finger joint behavior of the laminations in bending tests depending on the adhesive type. Variable mesh size, with a gradient ranging from 30 to 3 mm (decreasing close to the finger-joint proximities) at a maximum growth rate of 1.45, was employed (Fig. 4). Typical 4-point bending test following EN 408 specifications (CEN 2010) was simulated using geometrical models of laminations with dimensions of 70 mm- width, 22 mm-depth, and 396 mm-length. The applied loads were located on the central third and separated at 132 mm (see Fig. 2).

Timber was considered as an orthotropic and non-linear material, whose elastic–plastic behavior was modeled through the Comsol *hardening function* obtained from control tests. Input data of the physical and mechanical properties were obtained from the experimental tests on the control samples (see 3.1.), and other relevant properties derived from the empirical equations established in EN 384 (CEN 2016a) for deciduous species (Eqs. 3, 4, 5, 6, 7, 8 and 9).

$$E_{90} = E_0/15 \quad (3)$$

$$G = E_0/16 \quad (4)$$

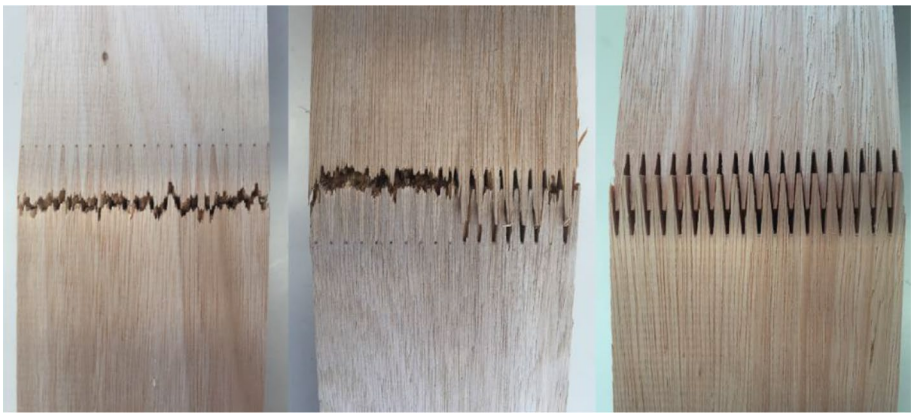

Fig. 3 Failure modes of finger-joint laminations: Mode 1 (left), Mode 2 (center) and Mode 3 (right)

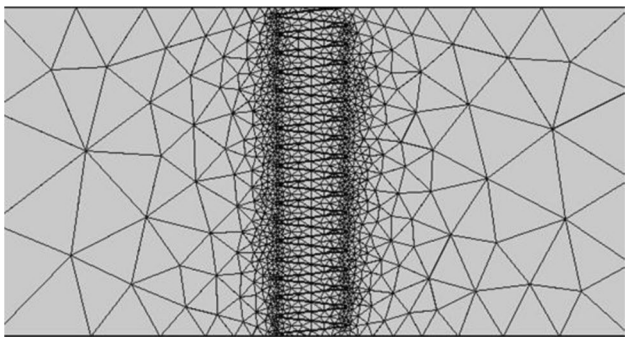

Fig. 4 Meshing of sample on the Finite Element model

$$f_{t,0} = 0.6 \cdot f_m \tag{5}$$

$$f_{t,90} = 0.6 \tag{6}$$

$$f_{c,0} = 5 \cdot (f_m)^{0.45} \tag{7}$$

$$f_{c,90} = 0.015 \cdot \rho \tag{8}$$

$$f_v = 4 \tag{9}$$

where, E_{90} is the modulus of elasticity perpendicular to the grain, E_0 is the modulus of elasticity parallel to the grain, obtained from experimental bending tests, G is the shear modulus, $f_{t,0}$ is the strength in tension parallel to the grain, $f_{t,90}$ is the strength in tension perpendicular to the grain, $f_{c,0}$ is the strength in compression parallel to the grain, $f_{c,90}$ is the strength in compression perpendicular to the grain, f_v is the shear strength, f_m is the bending strength, obtained from experimental bending tests.

Adhesive-wood interaction in the finger joints was modeled through the Comsol *Thin Elastic Layer* module, defined by the elastic properties of the adhesives, shown in Table 1. Young`s modulus and Poisson coefficients were taken from Stoeckel et al. (2013), de Castro San Román (2005), and Konnerth et al. (2007), respectively. Shear modulus was determined by Eq. 10 (Konnerth et al. 2007).

Table 1 Adhesive properties used in FE simulations

	Property/Adhesive type	PUR	EPI
Young`s modulus (GPa)	E_{ad}	0.50	3.50
Poisson coefficient	ν_{ad}	0.30	0.30
Shear modulus (GPa)	G_{ad}	0.19	1.35

$$G = E_{ad}/2 * (1 + \nu_{ad}) \tag{10}$$

where E_{ad} is the Young`s modulus of the adhesive, and ν_{ad} is the Poisson coefficient of the adhesive.

3 Results and discussion

3.1 Control samples

Experimental data of bending properties and density (E_0, f_m, and ρ), plus other derived mechanical properties (G, $f_{t,0}$, $f_{c,0}$, $f_{c,90}$ and f_v) from control samples, are shown in Table 2. Control samples were used as input data for FE modelling to predict the load–deflection curve in the elastic phase, without influence of the finger joints or the adhesive type. Control sample also provided input data to define the hardening function used in Comsol for the elastoplastic phase.

3.2 Experimental results of finger-joint laminations

Mean values of modulus of elasticity and bending strength recorded for each failure mode (i.e., 1, 2, and 3, as described in 2.2), were obtained from the three experimental samples: (i) control laminations without finger joints (hereinafter referred to as "controls"); (ii) glued finger joints with EPI

Table 2 Wood properties used in FE simulations. Mean values

E_0	f_m [a]	ρ [a]	E_{90} [b]	G [b]	$f_{t,0}$ [b]	$f_{c,0}$ [b]	$f_{t,90}$ [b]	$f_{c,90}$ [b]	f_v [b]
15,363 (15%)	91.9 (19%)	556 (12%)	1024	960	55.1	38.2	0.6	8.3	4.0

Values in parentheses indicate COV

Property values are in N/mm^2, with the exeption of ρ, which is in kg/m^3

[a]Experimental values from control samples

[b]Derived values from Eqs. 3, 4, 5, 6, 7, 8 and 9

(hereinafter referred to as "fj-EPI"); and (iii) glued finger joints with PUR (hereinafter referred to as "fj-PUR"). Table 3 shows mean properties and failure modes under bending tests for the three samples.

Percentage of failure in mode 1 was inferior to those corresponding to modes 2 and 3. In both samples (fj-EPI and fj-PUR), low percentages (25% in fj-EPI and 20% in fj-PUR) of failure in mode 1 (i.e., 100% wood) were observed.

Considering the whole sample, controls presented a significantly higher mean value of modulus of elasticity compared to those of fj-EPI and fj-PUR, being the last two, similar to each other. Focusing on the failure mode, significant differences between fj-EPI and fj-PUR were observed, but just for specimens that failed by adhesive (mode 3). Note that the modulus of elasticity, evaluated in the elastic phase of the load–deflection curve, is not affected by the ultimate load. However, failure by adhesive (mode 3) can occur in the elastic phase, affecting the modulus of elasticity depending on the adhesive type.

Typical load–deflection curves for laminations glued with EPI or glued with PUR, against controls (i.e., without finger joint) are depicted in Fig. 5.

As can be observed, the peak load attained in finger-jointed laminations was lower than in controls. While failure of controls occurred in the elastic–plastic phase, failure of finger-jointed samples appeared close to the yield limit, shown in Fig. 4 as the inflection point of the curves. Bending strength was significantly higher in fj-PUR ($f_m = 72.1$ N/mm^2) compared to that observed in fj-EPI ($f_m = 59.9$ N/mm^2), being both, lower than controls ($f_m = 91.9$ N/mm^2). These findings were higher than those reported by Piter et al. (2007) for finger joint laminations of Argentinean *E. grandis* glued with melamine-urea–formaldehyde adhesive (f_m between 46.9 and 49.7 N/mm^2).

Boxplots of bending properties by failure mode for controls and finger-jointed samples are shown in Fig. 6.

Analysis of $E_{0,mean}$ by failure mode within each fj-EPI and fj-PUR sample reveals an increasing trend of mean values from mode 1 to mode 3 (Fig. 6).

Similarly, bending strength in regard to failure mode within each fj-EPI and fj-PUR sample shows an increase in f_m from failure mode 1 to failure mode 3. The lowest bending strength observed in specimens that failed 100% by wood (mode 1) could mislead interpretations by contradicting the

Table 3 Experimental bending results of the three samples (mean values)

Sample			(i) Control	(ii) fj-EPI	(iii) fj-PUR
Specimens per sample (n)			20	20	20
Moisture content (%)			11.0 (±4%)	9.1 (±4%)	9.1(±3%)
$E_{0,mean}$ (kN/mm^2)			15.4[a] (±15%)	12.0[b] (±18%)	13.3[b] (±22%)
Failure mode 1 (wood)	$E_{0,mean\_1}$		15.4[a] (±15%)	10.6[b] (±17%)	11.6[b] (±15%)
Failure mode 2 (mixed)	$E_{0,mean\_2}$		15.4[a] (±15%)	12.1[b] (±19%)	12.3[b] (±21%)
Failure mode 3 (adhesive)	$E_{0,mean\_3}$		15.4[a] (±15%)	12.3[b] (±15%)	15.5[a] (±17%)
f_m (N/mm^2)			91.9[a] (±19%)	58,7[b] (±15%)	72.1[b] (±14%)
Failure mode 1 (wood)	f_{m_1}		91.9[a] (±19%)	53,5[b] (±12%)	60.9[b] (±5%)
Failure mode 2 (mixed)	f_{m_2}		91.9[a] (±19%)	58.8[b] (±10%)	69.5[b] (±9%)
Failure mode 3 (adhesive)	f_{m_3}		91.9[a] (±19%)	62.3[b] (±12%)	79.2[a] (±11%)
		n	Failure mode percentage		
Failure mode 1 (wood)		4	100% (n = 20)	25% (n = 5)	20% (n = 4)
Failure mode 2 (mixed)		7		40% (n = 8)	35% (n = 7)
Failure mode 3 (adhesive)		9		35% (n = 7)	45% (n = 9)

Values in parentheses indicate the coefficient of variation (CoV)

Within a row, different lowercase letters denote significant differences between control, EPI and PUR values with a confidence level of 95%

Failure mode 1: 100% wood; Failure mode 2: mixed; Failure mode 3: 100% adhesive

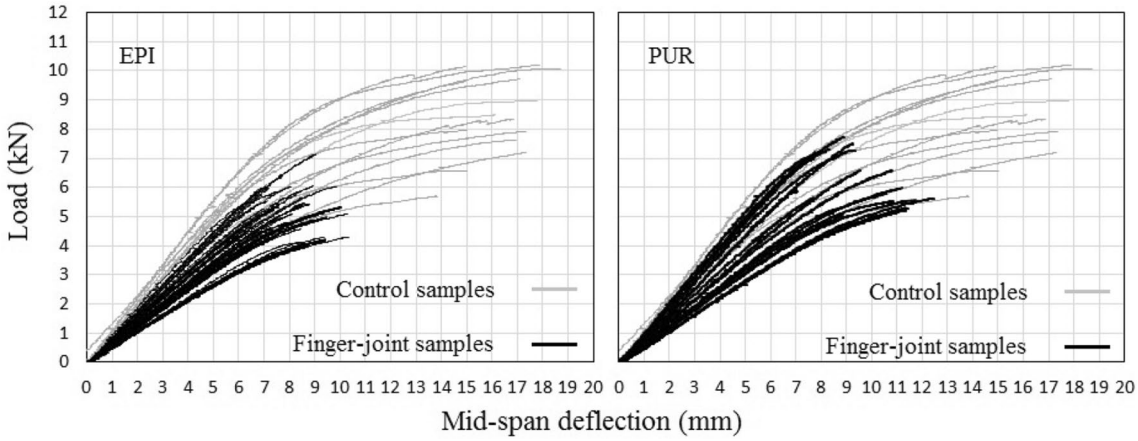

Fig. 5 Load-mid-span deflection curves of finger-jointed samples with EPI (left) and PUR (right) adhesive compared to control sample curves (grey color)

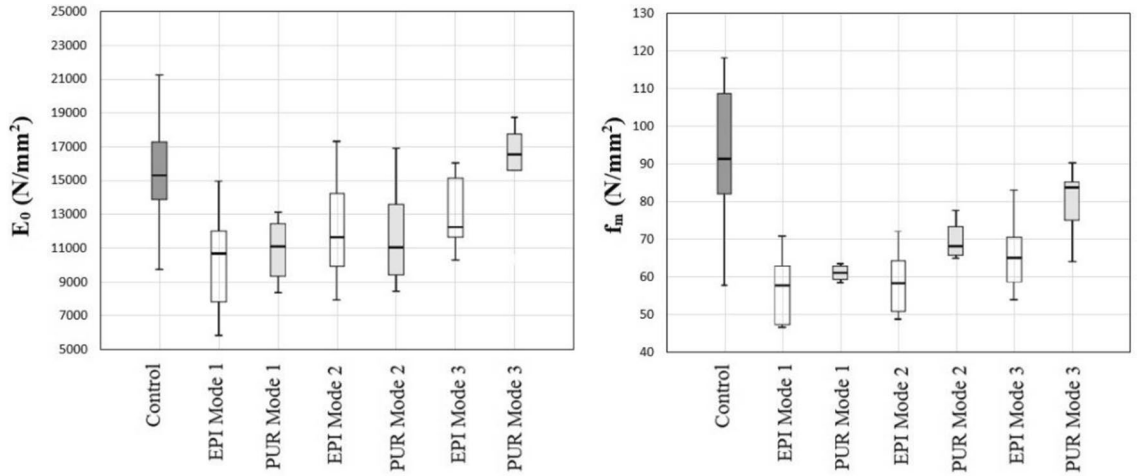

Fig. 6 Modulus of elasticity and bending strength by adhesive type and failure mode

premise that the finger joint is a weak point. However, this behavior could be attributed to wood heterogeneity, masking its influence on the bending strength and showing failure modes by adhesive.

Comparison of strength values between fj-EPI and fj-PUR, for failure mode 1 (56.47 and 60.88 N/mm^2, respectively), showed no significant differences, agreeing with the fact that the limiting factor was the wood strength rather than the glue line. On the other hand, significantly superior values of f_m in fj-PUR compared to fj-EPI for failure modes 2 and 3 were observed.

3.3 Validation of FE model

Typical load–deflection curves comparing the experimental results and the numerical predictions for control samples are presented in Fig. 7.

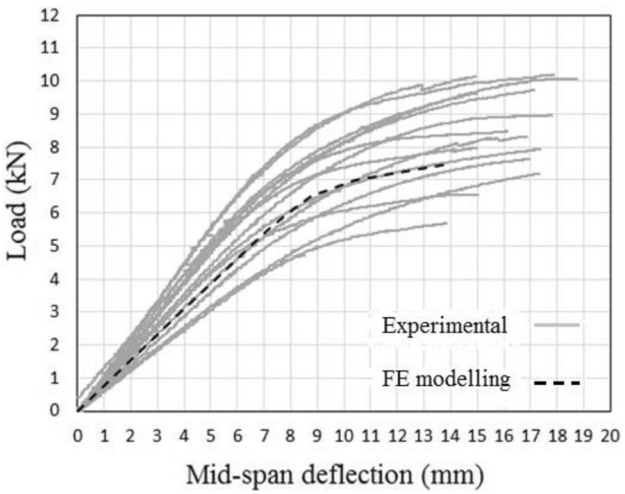

Fig. 7 Load-mid-span deflection curves for experimental and numerical control samples

As can be seen, the load–deflection curve obtained from the FE simulation matches the experimental curves. The numerical modulus of elasticity in the elastic phase resulted in 13.4 kN/mm^2, 12.5% lower than the experimental mean value, yet in between the minimum–maximum experimental range.

In addition, two numerical models to simulate the experimental behavior of finger-jointed laminations, one glued with EPI (fj-EPI), and one glued with PUR (fj-PUR), under bending tests were developed. Figure 8 presents the load–deflection curves obtained from the models in comparison with the experimentals.

The different adhesive (EPI and PUR) properties considered in the model had no significant influence on the numerical deflections and therefore, neither on the numerical modulus of elasticity. The adjustment of the numerical models was in good agreement with the experimental data. Table 4 shows the relative differences between the modulus of elasticity obtained from the numerical models and the mean values from experimental tests. A maximum error of 7.5% was observed for fj-PUR sample.

Once the model was validated for stiffness prediction, the next step involved applying the model to predict the bending strength of finger-jointed laminations. In doing so, based on the experimental results and considering an ideal behavior with proper adhesion of the finger-joints, two assumptions were alleged: (i) the glue line is stronger than the wood leading to a 100%-wood failure (mode 1); and (ii) the 5th percentile (characteristic value that reflects material variability) is similar for the whole sample, even in a hypothetical scenario where every finger-joint fails by mode 1 (leading to an increase of the *fm* mean value).

Bearing in mind that failure of laminations under bending typically occurs in the tensile side, the bending strength was estimated by evaluation of the tensile stress distributions of wood, in the vicinity of the finger-joints. The predicted strengths were compared with experimental results of specimens that failed in mode 1.

Table 4 Modulus of elasticity (E0) of finger-jointed laminations obtained from numerical modelling and experimental testing

	FE model	fj-EPI[a]	fj-PUR[a]	[fj-EPI + fj-PUR][a]
E_0 (mean value, kN/mm^2)	12.3	12.0	13.3	12.7
Error (%)	–	2.6	7.5	2.7

[a]Values obtained in experimental testing

Figure 9 shows the distribution of tensile stresses, parallel and perpendicular to the grain, in the proximities of the finger joints, obtained from the numerical models. The maximum stresses were observed close to the bottom of the fingers, coinciding with the rupture zone of the experimental specimens.

As expected, the tensile strength was higher in the direction parallel- than perpendicular- to the grain and therefore, the finger-joint failure occurred when the longitudinal tension stress at the bottom of the finger exceeded the estimated strength in tension parallel to the grain ($f_{t,0}$ = 55.1 N/mm^2) of *Eucalyptus grandis* (see Sect. 3.1). The peak load was determined for the first node that reached the value of $f_{t,0}$, and the numerical bending strength was calculated by Eq. 2. Table 5 shows the error in the prediction of the bending strength by FEM in comparison with the experimental values.

The numerical bending strength showed 6–17% lower values than the experimental means. Comparing the numerical results with the 5th percentile of experimental f_m, the estimation error is reduced to 4%. This decrease could be attributed to the way in which $f_{t,0}$ was calculated, *i.e.*, by the equation specified in EN 338 (CEN 2016b), which, due to safety reasons is conservative-oriented, instead of using

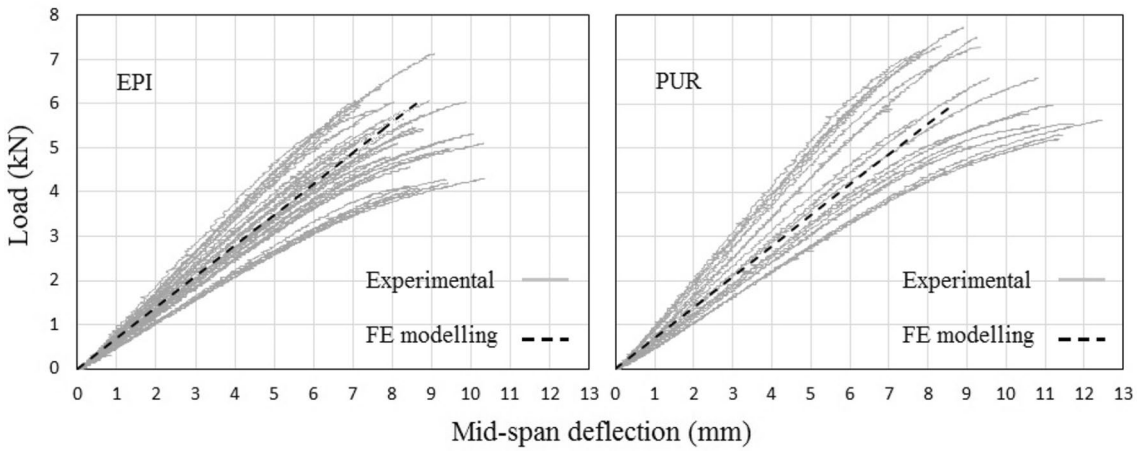

Fig. 8 Load-mid-span deflection curves of experimental samples vs. FE models

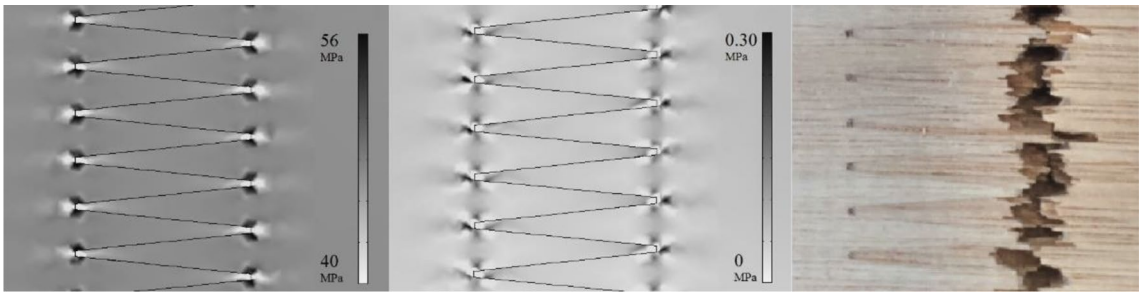

Fig. 9 Stress distributions (N/mm^2) parallel (left) and perpendicular (center) to the grain from FE modelling, and experimental failure (right) under bending load

Table 5 Bending strength (f_m) of finger-jointed laminations obtained from numerical modelling and experimental testing

	FE model	fj-EPI	fj-PUR	[fj-EPI+fj-PUR]	[fj-EPI+fj-PUR]	
f_m (mean value, N/mm^2)	50.3	53.5	60.9	60.4	f_{05} (5th percentile)	48.2
Error (%)	–	6.1	17.4	16.8		4.3

Table 6 Finger joint geometries evaluated by FEM

Finger code	Finger length l (mm)	Pitch p (mm)	Tip thickness b_t (mm)
10/4/0.5	10	4.0	0.5
11/4/0.5	11	4.0	0.5
13/4/0.5	13	4.0	0.5
15/4/0.5	15	4.0	0.5
20/5/0.5	20	5.0	0.5
20/6/1.0	20	6.2	1.0
30/6/1.0	30	6.2	1.0

experimental data. Nevertheless, it is worth noting that employing the mechanical properties derived by EN 338 (CEN 2016b) equations leads to a reasonable prediction of the bending strength from *Eucalyptus grandis* finger-joints.

Since the finger geometry has a relevant effect on the performance of the structural joints (Bustos et al. 2003; Tran et al. 2015), several finger-joint geometries were considered in FE modeling. The strength performance of the different geometries was evaluated just for mode 1, where failure occurs due to tension stresses in wood, rather than adhesive (failure modes 2 and 3), where the modelling of the wood-adhesive interaction becomes unpredictable. Table 6 shows the finger-joint geometries evaluated according to the common lengths used in Argentina and Uruguay (10–15 mm) and others reccommended by EN 14080:

Finger lengths of 15, 20 and 30 mm (with their corresponding values of pitch and tip thickness) indicated in EN 14081 and, lengths of 10, 11 and 13 mm, usually employed in Uruguayan industries, were considered. The modelling parameters were similar to those defined in 2.3. The estimated bending strength obtained for each finger-joint geometry is shown in Fig. 10:

As can be seen, the numerical bending strength slightly improved by increasing the finger length; results that compare relatively well with those obtained from tests for fingers with codes 10/4/0.5, 11/4/05 and 13/4/05. As was previously mentioned, the improvement in strength is related to the different distribution of tensile stresses near the bottom of the finger, being valid just for failure mode 1. Increasing the length of the finger entails an augmentation of the contact area between wood and adhesive, which in turn should improve mode 2 and 3 results. Results showed that lower bending strength values (and therefore defining the characteristic values) were obtained in samples with failure mode 1. Under this premise, the evaluation of different geometries by FEM indicates that a finger length of 20 mm is optimal for maximizing the bending strength for failure mode 1.

3.4 Conclusion

Eucalyptus grandis finger-joints glued with different adhesives (PUR and EPI) were tested in bending to obtain their mechanical properties and to evaluate the failure mode. Additionally, numerical simulations were developed to model the finger-joints and to estimate their strength and stiffness.

The experimental tests showed no significant differences in the modulus of elasticity (E_0) for laminations with finger-joints glued with EPI and with PUR, being both significantly lower than those from controls (laminations without finger-joint). However, the bending strength (f_m) of finger-joints was significantly higher for PUR than for EPI, being both

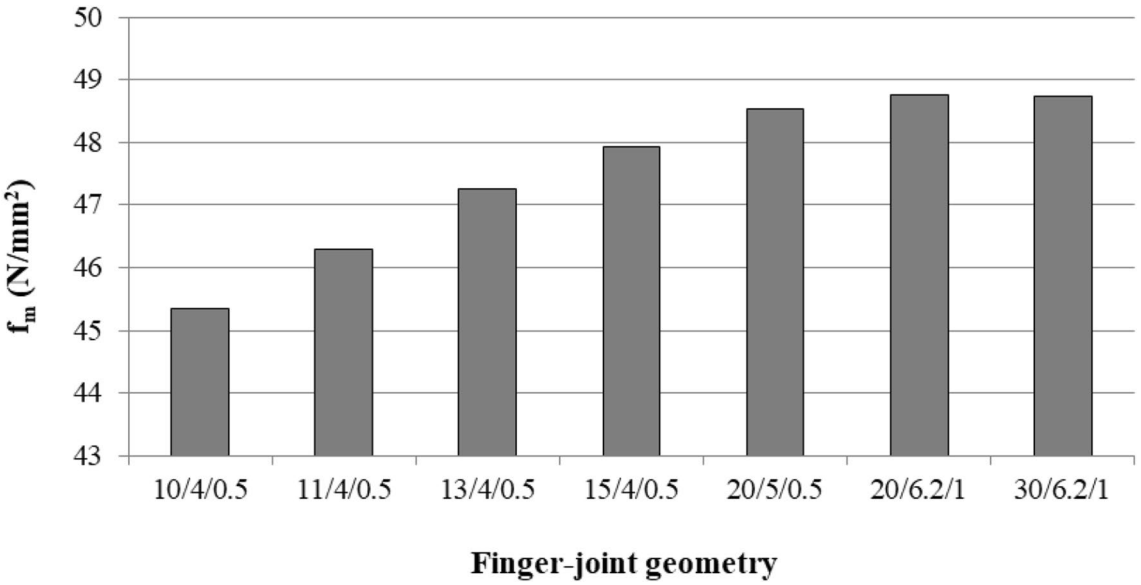

Fig. 10 Bending strength f_m (N/mm^2) of different finger-joint geometries estimated by FEM

lower than controls. In the present work, the lowest bending properties obtained in samples with failure mode 1 (failure 100% by wood) suggests that the characteristic strength value of finger joints was defined by the mechanical properties of wood and not by the quality of the finger joint.

Despite the relatively high values of bending strength reached in the finger-joints, high percentages of undesirable failure type, *i.e.*, in the glue line (modes 2 and 3) for both adhesives (75% in EPI samples and 80% in PUR samples), were found. This observation suggests that the wood-adhesive interphase has yet to be improved, probably by optimizing the manufacturing parameters or evaluating the performance of new adhesives.

There were no differences in the numerical results for the modelling of the laminations as a function of the type of adhesives used for the gluing of the finger joints. The numerical modulus of elasticity of finger-joint laminations was estimated with a maximum error of 7.5% with respect to the experimental mean values. From these models, bending strength could be predicted in a conservative way, with an error of 4.3% compared with the experimental value of the 5th percentile.

FEM modelling showed that optimum finger geometry is 20 mm length, with a gap of 6.2 mm and tip thickness of 1 mm. This finger configuration maximizes the bending strength in failure modes 1 and, therefore, the characteristic value.

In further works, the accuracy of the numerical models for bending strength prediction could be improved by using experimental data as input values for the entire set of elastic and mechanical properties needed. In addition, more complex FE models considering the interaction between wood and adhesive for modelling failure modes 2 and 3, should be developed.

Acknowledgments The authors thank the National Agency for Research and Innovation (ANII) of Uruguay for the funds for the execution of this project (PR FSA_1_2013_1_12897) and for the funds for the postdoctoral fellowship of Dr. Abel Vega in the *Facultad de Ingeniería, Universidad de la República* (PD_NAC_2014_1_102147).

Compliance with ethical standards

Conflict of interest On behalf of all authors, the corresponding author states that there is no conflict of interest.

References

Ahmad Z, Lum WC, Lee SH et al (2017) Mechanical properties of finger jointed beams fabricated from eight Malaysian hardwood species. Constr Build Mater 145:464–473. https://doi.org/10.1016/j.conbuildmat.2017.04.016

Ayarkwa J, Sasaki HYY (2000a) Effect of finger geometry and end pressure on the flexural properties of finger-jointed tropical African hardwoods. For Prod J 50(11–12):53–63

Ayarkwa J, Hirashima Y, Sasaki Y, Ando K (2000b) Effect of glue type on flexural and tensile properties of finger-jointed tropical African hardwoods. For Prod J 50(10):59–68

Bourreau D, Aimene Y, Beauchene J, Thibaut B (2013) Feasibility of glued laminated timber beams with tropical hardwoods. Eur J Wood Prod 75:653–662

Bourscheid CB, Terezo RF, Stüpp AM, Vanzella DA (2015) Desempenho mecânico de madeira laminada colada de Eucalyptus spp. [Mechanical performance of Eucalyptus spp. glulam] In: Anais do I I Congresso Brasileiro de Ciencia e Tecnologia da Madeira - CBCTEM. Belo Horizonte, Brazil

Bustos C, Mohammad M, Hernández RE, Beauregard R (2003) Effects of curing time and end pressure on the tensile strength of finger-jointed black spruce lumber. For Prod J 53:85

Calil Neto C, Christoforo AL, Ribeiro Filho SM et al (2014) Evaluation of strength to shear and delamination in glued laminated wood. Ciência Florest 23:989–996

Camú CT, Aicher S (2018) A stochastic finite element model for glulam beams of hardwoods. In: World conference on timber engineering. Seoul, South Korea

CEN (2013) EN 14080. Timber structures. Glued laminated timber and glued solid timber. Requirements. CEN/TC 124/WG3. Brussels

CEN (2015) EN 16351. Timber structures. Cross laminated timber. Requirements. CEN/TC 124/WG 3, Brussels

CEN (2010) EN 408. Timber structures. Structural timber and glued laminated timber. Determination of some physical and mechanical properties. CEN/TC 124/WG1, Brussels

CEN (2016a) EN 384. Structural timber. Determination of characteristic values of mechanical properties and density. CEN/TC 124/WG2, Brussels

CEN (2016b) EN 338. Structural timber. Strength classes. CEN/TC 124/WG2. Brussels **P**

de Castro San Román J (2005) Experiments on Epoxy, Polyurethane and ADP adhesives: composite construction laboratory, Technical Report Nr. CCLab2000.1b/1

Dieste A (2012) Programa de promoción de exportaciones de productos de madera [Wood Products Export Promotion Program] Dirección Nacional de Industrias, Ministerio de Industrias, Energía y Minería, Consejo Sectorial Forestal-Madera [National Direction of Industries, Ministry of Industries, Energy and Minning, Forest-Wood Sectorial Council]. p 38

Franke B, Schusser A, Müller A (2014) Analysis of finger joints from beech wood. In: World conference on timber engineering. Quebec, Canada

Franke S, Marto J (2014) Investigation of *Eucalyptus globulus* wood for the use as engineered wood material. In: Proceedings of the world conference on timber engineering. Quebec, Canada

Milner HR, Yeoh E (1991) Finite element analysis of glued timber finger joints. J Struct Eng 117:755–766

IRAM (2013a) IRAM 9661:2013. Madera laminada encolada estructural. Requisitos de fabricación de los empalmes por unión dentada [Glued laminated timber. Requirements of manufacturing of the finger joints]. Instituto Argentino de Normalización y Certificación-IRAM- [Argentinean Institute of Standardization and Certification], Buenos Aires

IRAM (2006) IRAM 9660–1:2006. Madera laminada encolada estructural. Parte 1. Clases de resistencia y requisitos de fabricación y control [Glued laminated timber. Part 1. Strength classes and manufacturing and control requirements]. Instituto Argentino de Normalización y Certificación-IRAM- [Argentinean Institute of Standardization and Certification], Buenos Aires

IRAM (2013b) IRAM 9662-2: 2013. Madera laminada encolada estructural. Clasificación visual de las tablas por resistencia. Parte 2. Tablas de Eucalyptus grandis [Glued laminated timber. Visual grading of boards by strength. Part 2. Boards of Eucalyptus grandis]. Instituto Argentino de Normalización y Certificación-IRAM- [Argentinean Institute of Standardization and Certification], Buenos Aires

Iwakiri S, Monteiro Matos JL, Prata JG et al (2014) Characteristics of glued laminated beams made of teak wood (*Tectona grandis*). Floresta e Ambient 21:269–275

Khelifa M, Auchet S, Méausoone PJ, Celzard A (2015) Finite element analysis of flexural strenghening of timber beams with Carbon Fibre-Reinforced Polymers. Eng Struct 101:364–375

Konnerth J, Gindl W, Müller U (2007) Elastic properties of adhesive polymers. I. Polymer films by means of electronic speckle pattern interferometry. J Appl Polym Sci 103:3936–3939. https://doi.org/10.1002/app.24434

Lara-Bocanegra AJ, Majano-Majano A, Crespo J, Guaita M (2017) Finger-jointed Eucalyptus globulus with 1C-PUR adhesive for high performance engineered laminated products. Constr Build Mater. https://doi.org/10.1016/j.conbuildmat.2017.01.004

Moya L, Pérez-Gomar C, Vega A, Sánchez A, Torino I, Baño V (2019) Relationship between manufacturing parameters and structural properties of *Eucalyptus grandis* glued laminated timber. Maderas 21:21

Özçifçi AYF (2008) Structural performance of the finger-jointed strength of some wood species with different joint configurations. Constr Build Mater 22:1543–1550

Pereira MC, Calil Neto C, Icimoto FH, Calil Junior C (2016) Evaluation of tensile strength of a Eucalyptus grandis and *Eucalyptus urophyla* Hibrid in wood beams bonded together by means of finger joints and polyurethane-based glue. Mater Res 19:1270–1275

Piter JC, Cotrina AD, Sosa Zitto MA et al (2007) Determination of characteristic strength and stiffness values in glued laminated beams of Argentinean *Eucalyptus grandis* according to European standards. Holz Roh- Werkst 65:261–266. https://doi.org/10.1007/s00107-006-0161-5

Raknes E (1980) The influence of production conditions on the strength of finger-joints (of sawnwood in Norway). In: Transmitted by the Government of Norway in FAO, Geneva (Switzerland). Joint ECE/FAO Agriculture and Timber Div. Seminar on the PRoduction, Marketing and Use of Finger-Jointed Sawnwood. Hamar (Norway)

Sebera V, Muszyński L, Tippner J et al (2015) FE analysis of CLT panel subjected to torsion and verified by DIC. Mater Struct 48:451–459. https://doi.org/10.1617/s11527-013-0195-1

Serrano E, Gustafsson J, Larsen HJ (2001) Modeling of finger-joint failure in glued-laminated timber beams. J Struct Eng 127:914–921

Smardzewski J (1996) Distribution of stresses in finger joints. Wood Sci Technol 30:477–489

Stoeckel F, Konnerth J, Gindl-altmutter W (2013) Mechanical properties of adhesives for bonding wood—a review. Int J Adhes Adhes 45:32–41

Tran VD, Oudjene M, Méausoone PJ (2015) Experimental and numerical analysis of the structural response of adhesively reconstituted beech timber beams. Compos Struct 119:206–217

Tran VD, Oudjene M, Méausoone PJ (2014) FE analysis and geometrical optimization of timber beech finger-joint under bending test. Int J Adhes Adhes 52:40–47. https://doi.org/10.1016/j.ijadhadh.2014.03.007

Vassiliou V, Barboutis I, Karastergiou S (2006) Effect of PVA bonding on finger-joint strength of steamed and unsteamed beech wood (*Fagus sylvatica*). J Appl Polym Sci 103:1664–1669

Volkmer T, Schusser A, Franke B (2014) Analysis of the penetration of adhesives at finger-joints in beech wood. In: WCTE 2014 World Conference on Timber Engineering, Quebec, Canada. August 10-14 2014

Vrazel M, Sellers Jr T (2004) The effects of species, adhesive type and cure temperature on the strength and durability of a structural finger-joint. For Prod J 54:66–75